

# A new variational approach for the Holstein Molecular Crystal Model

V. Cataudella, G. De Filippis and G. Iadonisi

<sup>†</sup>*Dipartimento di Scienze Fisiche, Università di Napoli I-80125 Napoli, Italy*

(May 20, 2018)

A new variational technique is developed to investigate the polaronic features of the Holstein Molecular Crystal Model. It is based on a linear superposition of Bloch states that describe large and small polaron wave functions. It is shown that this method provides a very good description of the regime characterized by intermediate values of the electron-phonon coupling constant (the so-called intermediate polaron) for any value of the adiabatic parameter  $\omega_0/t$ . The polaron ground state energy in one and two dimensions is calculated and successfully compared with the best estimates available providing a clear physical interpretation of the intermediate polaron. The band structure, the spectral weight of the ground state and the lattice displacement associated to the polaron are also calculated and discussed. The new method has the advantage to require a very little computational effort.

## I. INTRODUCTION

Recently a large amount of experimental results, ranging from infrared spectroscopy to transport properties involving the colossal magneto-resistance and high  $T_c$  superconductivity, has pointed out the presence of polaronic carriers in doped cuprates and in the manganese oxide perovskites<sup>1,2</sup>. In particular several experiments have shown that in doped perovskite manganites  $La_{1-x}A_xMnO_3$  ( $A = Sr, Ca$ ) there is a quite considerable coupling between the charge and the lattice degrees of freedom<sup>2</sup>. The lattice distortions associated with the  $Mn$  ions play an important role in determining the electronic and magnetic properties of these compounds which have become the focus of the scientific interest after the discovery of the colossal magneto-resistance phenomena. Recently it has been found that in  $La_{0.75}Ca_{0.25}MnO_3$  the metallic phase is characterized by homogeneously distributed intermediate polarons while, above the transition from ferromagnetic metal to paramagnetic insulator, small and intermediate polarons coexist<sup>3</sup>. Also the measurements of the  $CuO$  distances in  $La_{1.85}Sr_{0.15}CuO_4$  crystal have pointed out, below 100K, two conformations of the  $CuO_6$  octahedra assigned to two different types of polarons<sup>4</sup>.

This large amount of experimental data has renewed the interest in studying the models of the electron-phonon coupled system and in particular the Holstein molecular crystal model that, for his relative simplicity, is the most considered model for the interaction of a single tight-binding electron coupled to an optical local phonon mode<sup>5</sup>.

For the Holstein hamiltonian, beside the weak-coupling perturbative theory<sup>6</sup> an analytical approach is known for the strong coupling limit in the nonadiabatic regime (small polaron)<sup>7</sup>. It is based on the Lang-Firsov canonical transformation and on expansion in powers of  $1/\lambda$  where  $\lambda = E_p/zt$  is the dimensionless coupling constant,  $E_p$ ,  $z$  and  $t$  being, respectively, the small polaron binding energy, the coordination lattice number and the bare effective hopping integral ( $\lambda$  represents the ratio between the small polaron binding energy and the energy gain of an itinerant electron on a rigid lattice). It is well known that both these analytical techniques fail to describe the region, of greatest physical inter-

est, characterized by intermediate couplings and by electronic and phononic energy scales not well separated. This regime has been analyzed in several works based on Monte Carlo simulations<sup>8,9</sup>, numerical exact diagonalization of small clusters<sup>10</sup>, dynamical mean field theory<sup>11</sup>, density matrix renormalization group<sup>12</sup> and variational approaches<sup>13,14</sup>. The general conclusion is that the ground state energy and the effective mass in the Holstein model are continuous functions of the electron-phonon coupling and that there is not phase transition in this one-body system<sup>15</sup>. In particular when the interaction strength is greater than a critical value the ground state properties change significantly but without breaking the translational symmetry.

Recently, results for the Holstein molecular crystal model have been presented by using the Global-Local variational method<sup>13</sup>. The comparison of the data obtained in one space dimension with the known approaches has shown that these results seem to provide the best estimates of the polaron ground state energy. They are highly accurate over a wide range of the polaron parameter space, from the non-adiabatic to the adiabatic, from weak to strong coupling limit. Nevertheless a solution of the Global-Local variational method for any particular  $k$  value ( $k$  is the wave number of the polaron Bloch state) is obtained by minimizing with respect to a very large number of parameters, that depends on the number of lattice sites and that increases dramatically with increasing the number of space dimensions from one to three.

The aim of this work is to study the Holstein polaron features including ground state energy, polaron energy band, shape of the lattice distortion induced by the electron-phonon interaction and spectral weight of the coherent polaron band within a new variational approach. It is based on two translationally invariant Bloch wave functions that provide a very good description of the two asymptotic regimes, the weak and strong coupling regimes. In this paper these wave functions are called large and small polaron. In the large polaron wave function the phonon distribution function takes into account the average effect of the correlation among the emission of successive virtual phonons by the electron and the spatial extension of the polaron is large compared with the lattice parameter of the crystal. In the

small polaron wave function the lattice polarization is confined to a region of the order of the unit cell and the polaron radius becomes of the order of the lattice constant. In this case all momenta of the Brillouin zone contribute to the polaron wave function and in the phonon distribution function the effect of the electron recoil due to the emission of virtual phonons is negligible.

A careful inspection of these two wave functions points out that, far away from the two asymptotic regimes, they are not orthogonal and that the off-diagonal matrix elements of the Holstein hamiltonian are not zero. It is then straightforward to determine variationally the polaron ground state energy by considering as trial state the linear superposition of the large and small polaron wave functions.

The comparison of our results with the Monte Carlo<sup>9</sup> data and the ground state energies of the variational global local method<sup>13</sup> shows that the proposed method provides a very good description of the polaron ground state energy for any value of the parameters of the Holstein model and confirms the existence of three regimes<sup>13</sup>: the weak coupling regime, characterized by polaron masses lightly heavier than the free electron mass and by dimension of the lattice polarization large compared with the lattice parameter; the strong coupling regime where the well-known polaronic band collapse takes place and the intermediate regime that is characterized by the crossover between the small and large polaron solutions. This regime is, therefore, well described by a wave function that is a linear superposition of Bloch states that describe the small and large polaron.

We stress that the new variational approach provides a clear description of the Holstein polaron features in any regime and involves, for any particular  $k$  value, a very small number of variational parameters, that does not depend on the number of lattice sites.

## II. A NEW VARIATIONAL WAVE FUNCTION

**The model.** The Holstein molecular crystal model is described by the Hamiltonian<sup>5</sup>:

$$H = H_{el} + H_{ph} + H_I = -t \sum_{} c_i^\dagger c_j + \omega_0 \sum_{\vec{q}} a_{\vec{q}}^\dagger a_{\vec{q}} + \sum_{i,\vec{q}} c_i^\dagger c_i \left[ M_q e^{i\vec{q} \cdot \vec{R}_i} a_{\vec{q}} + h.c. \right]. \quad (1)$$

The units are such that  $\hbar = 1$ . Since we will restrict ourselves to the single electron case we will not consider electron spin indices. The symbol  $<>$  in the first term of the sum in Eq.(1) means that the summation is to be carried out only when  $i$  and  $j$  are nearest neighbours to each other.

In the Eq.(1)  $c_i^\dagger$  denotes the electron creator operator at site  $i$ , the position vector of which is indicated by  $\vec{R}_i$ ,  $a_{\vec{q}}^\dagger$  represents the creation operator for phonon with wave number  $\vec{q}$ ,  $t$  is the transfer integral between nearest neighbor sites,  $\omega_0$  is the frequency of the optical local phonon mode and  $M_q$  indicates the electron-phonon matrix element. In the Holstein model (short range electron-phonon interaction)  $M_q$  assumes the form:

$$M_q = \frac{g}{\sqrt{N}} \omega_0. \quad (2)$$

Here  $N$  is the number of lattice sites.

### The small polaron

When the value of  $g$  is sufficiently large the lattice polarization cannot follow the electronic oscillations and, therefore, depends only on the average charge distribution of the electron. The wave function of the system can be factorized into a product of normalized variational functions  $|\varphi>$  and  $|f>$  depending on the electron and phonon coordinates respectively<sup>16</sup>:

$$|\psi^{(s)}> = |\varphi> |f> \quad (3)$$

where

$$|\varphi> = \sum_{\vec{R}_m} c_m^\dagger |0>_{el} \phi(\vec{R}_m) \quad (4)$$

and  $|f>$  has to be determined variationally.

In the Eq.(4)  $|0>_{el}$  is the electron vacuum state and  $\phi(\vec{R}_m)$  are variational parameters that satisfy the relation:

$$\sum_{\vec{R}_m} |\phi(\vec{R}_m)|^2 = 1 . \quad (5)$$

The expectation value of the Hamiltonian (1) on the state (3) gives:

$$\langle \psi^{(s)} | H | \psi^{(s)} \rangle = -t \sum_{\vec{R}_m, <\vec{\delta}>} \phi^*(\vec{R}_m) \phi(\vec{R}_m - \vec{\delta}) + \langle f | \sum_{\vec{q}} \left[ \omega_0 a_{\vec{q}}^\dagger a_{\vec{q}} + \rho_{\vec{q}} a_{\vec{q}} + \rho_{\vec{q}}^* a_{\vec{q}}^\dagger \right] | f \rangle \quad (6)$$

with

$$\rho_{\vec{q}} = M_q \sum_i e^{i\vec{q} \cdot \vec{R}_i} |\phi(\vec{R}_i)|^2 . \quad (7)$$

In the Eq.(6) the symbol  $<>$  in the summation means that  $\vec{\delta}$  runs only over the nearest neighbours.

The variational problem with respect to  $|f\rangle$  leads to the following lowest energy phonon state:

$$|f\rangle = e^{\sum_{\vec{q}} \left[ \frac{\rho_{\vec{q}}}{\omega_0} a_{\vec{q}} + h.c. \right]} |0\rangle_{ph}, \quad (8)$$

where  $|0\rangle_{ph}$  is the phonon vacuum state, and to the following total energy:

$$E_0 = -t \sum_{\vec{R}_m, <\vec{\delta}>} \phi^*(\vec{R}_m) \phi(\vec{R}_m - \vec{\delta}) - \sum_{\vec{q}} \frac{|\rho_{\vec{q}}|^2}{\omega_0} . \quad (9)$$

Even if this self-trapped state provides a good approximation of the ground state energy of the small polaron it is evident that the true eigenstate of the electron-lattice coupled system has translational symmetry. We construct translationally invariant Bloch states by taking a superposition of the localized states (3) centered on different lattice sites in the same manner in which one constructs a Bloch wave function from a linear combination of atomic orbitals. Then the trial wave function that accounts for the translational symmetry is given by (see also ref.17):

$$|\psi_{\vec{k}}^{(s)}\rangle = \frac{1}{\sqrt{N}} \sum_{\vec{R}_n} e^{i\vec{k} \cdot \vec{R}_n} |\psi_{\vec{k}}^{(s)}(\vec{R}_n)\rangle \quad (10)$$

where

$$|\psi_{\vec{k}}^{(s)}(\vec{R}_n)\rangle = \sum_{\vec{R}_m} c_{m+n}^\dagger |0\rangle_{el} \phi_{\vec{k}}(\vec{R}_m) e^{\sum_{\vec{q}} [f_{\vec{q}}(\vec{k}) a_{\vec{q}} e^{i\vec{q}\cdot\vec{R}_n} + h.c.]} |0\rangle_{ph} \quad (11)$$

and

$$f_{\vec{q}}(\vec{k}) = \frac{\rho_{\vec{q}}(\vec{k})}{\omega_0} = \frac{M_q}{\omega_0} \sum_{\vec{R}_m} |\phi_{\vec{k}}(\vec{R}_m)|^2 e^{i\vec{q}\cdot\vec{R}_m} . \quad (12)$$

This wave function is a sum of coherent states in the phonon coordinates, one for any particular lattice site. Since in a coherent state the emission of phonons occurs through a number of independent processes it is evident that in this trial state there is not correlation among the emission of successive virtual phonons. This physical assumption, i.e. that on every lattice site virtual phonons are emitted independently, is well-founded when  $g$  is sufficiently large but it is questionable for intermediate and small values of the electron-phonon interaction where the electron recoil kinetic energy plays an essential role. Moreover the wave function (10) does not contain states with real phonons. This indicates that the calculation of the polaron energy provides correct results only if the effective polaron band width  $\Delta$  and the phonon energy  $\omega_0$  satisfy the condition  $\Delta < \omega_0$ . As it is well known, both these approximations limit the validity of the wave function (10) to the strong coupling limit.

The expectation value of the Hamiltonian (1) on the state (10) gives:

$$\langle \psi_{\vec{k}}^{(s)} | H_{el} | \psi_{\vec{k}}^{(s)} \rangle = -t \sum_{\vec{R}_n} e^{i\vec{k}\cdot\vec{R}_n} e^{-\sum_{\vec{q}} |f_{\vec{q}}|^2 (1-e^{-i\vec{q}\cdot\vec{R}_n})} \sum_{\vec{R}_m, <\vec{\delta}>} \phi_{\vec{k}}^*(\vec{R}_m) \phi_{\vec{k}}(\vec{R}_m - \vec{R}_n - \vec{\delta}) \quad (13)$$

$$\begin{aligned} \langle \psi_{\vec{k}}^{(s)} | H_{ph} + H_I | \psi_{\vec{k}}^{(s)} \rangle &= \sum_{\vec{R}_n} e^{i\vec{k}\cdot\vec{R}_n} e^{-\sum_{\vec{q}} |f_{\vec{q}}|^2 (1-e^{-i\vec{q}\cdot\vec{R}_n})} \sum_{\vec{R}_m} \phi_{\vec{k}}^*(\vec{R}_m) \phi_{\vec{k}}(\vec{R}_m - \vec{R}_n) \\ &\quad \sum_{\vec{q}} \left[ |f_{\vec{q}}|^2 \omega_0 e^{-i\vec{q}\cdot\vec{R}_n} - f_{\vec{q}}^* M_q e^{i\vec{q}\cdot(\vec{R}_m - \vec{R}_n)} - f_{\vec{q}} M_q^* e^{-i\vec{q}\cdot\vec{R}_m} \right] . \end{aligned} \quad (14)$$

Moreover the calculation of the normalization factor  $\langle \psi_{\vec{k}}^{(s)} | \psi_{\vec{k}}^{(s)} \rangle$  gives:

$$\langle \psi_{\vec{k}}^{(s)} | \psi_{\vec{k}}^{(s)} \rangle = \sum_{\vec{R}_n} e^{i\vec{k}\cdot\vec{R}_n} e^{-\sum_{\vec{q}} |f_{\vec{q}}|^2 (1-e^{-i\vec{q}\cdot\vec{R}_n})} \sum_{\vec{R}_m} \phi_{\vec{k}}^*(\vec{R}_m) \phi_{\vec{k}}(\vec{R}_m - \vec{R}_n) . \quad (15)$$

The next step is the determination of the variational parameters  $\phi_{\vec{k}}(\vec{R}_n)$ . We note that if one neglects the spatial broadening of the electronic wave function, i.e.  $\phi_{\vec{k}}(\vec{R}_n) = \delta_{\vec{R}_n,0}$ , the Lang Firsov approximation is recovered, i.e. the exact solution of the Holstein molecular crystal model for  $\omega_0/t \rightarrow \infty$ . When the value of the adiabatic parameter  $\omega_0/t$  decreases it becomes necessary to go beyond this approximation. In this paper we assume:

$$\phi_{\vec{k}}(\vec{R}_n) = \alpha_{\vec{k}}\delta_{\vec{R}_n,0} + \beta_{\vec{k}}\delta_{\vec{R}_n,\vec{\delta}} + \gamma_{\vec{k}}\delta_{\vec{R}_n,\vec{\zeta}}. \quad (16)$$

Here  $\beta_{\vec{k}}$  and  $\gamma_{\vec{k}}$  are two variational parameters,  $\alpha_{\vec{k}}$  is determined in such a way the Eq.(5) is satisfied and  $\vec{\delta}$  and  $\vec{\zeta}$  indicate, respectively, the nearest and the next nearest neighbours.

This choice of the parameters  $\beta_{\vec{k}}$  and  $\gamma_{\vec{k}}$  that takes into account the broadening of the electronic wave function in every lattice site to the nearest neighbours and to the next nearest neighbours allows to obtain a variational estimate of the ground state energy at  $\vec{k} = 0$  that is lower than the result of the second order of the perturbation theory<sup>7</sup>:

$$E^{(sc)} \simeq E_p \left( 1 + \frac{1}{2z\lambda^2} \right) \quad (17)$$

where  $E_p$  indicates the small polaron binding energy to the first order of the perturbation theory:

$$E_p = - \sum_{\vec{q}} \frac{|M_{\vec{q}}|^2}{\omega_0} \quad (18)$$

and  $z$  is the nearest neighbour number. In appendix the calculation of the polaron band within the ansatz (16) for the variational parameters  $\phi_{\vec{k}}(\vec{R}_n)$  is reported.

We end this section noting that this method can be systematically improved by adding further terms in Eq.(16). This allows to obtain better and better estimates of the polaron energy in the strong coupling limit.

### The large polaron

It is well known that when the value of  $g$  is small the picture is quite different. As the electron moves through the crystal it exerts weak forces upon the ions which respond and move. This resultant ionic polarization will, in turn, modify the motion of the electron.

Then the particle must drag this polarization with it during its motion through the solid. This affects its effective mass that is weakly larger than that of a Bloch electron<sup>18</sup>. In this weak-coupling regime is useful to adopt a variational approach similar to that of Lee, Low and Pines in the continuum approximation<sup>19</sup>. A possible choice for the trial wave function is:

$$|\psi_{\vec{k}}^{(l)}\rangle = \frac{1}{\sqrt{N}} \sum_{\vec{R}_n} e^{i\vec{k}\cdot\vec{R}_n} |\psi_{\vec{k}}^{(l)}(\vec{R}_n)\rangle \quad (19)$$

where

$$|\psi_{\vec{k}}^{(l)}(\vec{R}_n)\rangle = c_n^\dagger |0\rangle_{el} e^{\sum_{\vec{q}} \left[ h_{\vec{q}}(\vec{k}) a_{\vec{q}} e^{i\vec{q}\cdot\vec{R}_n} + h.c. \right]} \left[ |0\rangle_{ph} + \sum_{\vec{q}} d_{\vec{q}}^*(\vec{k}) e^{-i\vec{q}\cdot\vec{R}_n} a_{\vec{q}}^\dagger |0\rangle_{ph} \right] \quad (20)$$

and

$$h_{\vec{q}}(\vec{k}) = \frac{M_q}{\omega_0 + E_b(\vec{q}) - E_b(\vec{q}=0)} \quad (21)$$

Here  $E_b(\vec{q})$  is the free electron band energy:

$$E_b(\vec{q}) = -2t \sum_{i=1}^d \cos(q_i a) \quad (22)$$

where  $a$  is the lattice parameter and  $d_{\vec{q}}(\vec{k})$  is a variational function that has to be determined by minimizing the expectation value of the Hamiltonian (1) on the state (19).

$|\psi^{(l)}(\vec{k})\rangle$  has the right translational symmetry, i.e. it is a Bloch state with wave number  $\vec{k}$ . This wave function represents an electron dressed by the virtual phonon field that describes the ionic polarization. We note that the term in the square brackets of the Eq.(20) allows a considerable advantage over the independent phonon approximation of Lee, Low and Pines. In the Lee, Low and Pines ansatz an important physical ingredient is missing: it does not take into account the fact that the polaron energy can approach  $\omega_0$ . On the contrary the wave function (19) contains this physical information<sup>20</sup>. In particular when the polaron excitation energy becomes equal to the energy of a longitudinal optical phonon, the band dispersion flattens and becomes horizontal. For these values of  $\vec{k}$  the band has the bare phonon-like behaviour with very small spectral weight. For the same values of  $\vec{k}$  and

in particular at the edges of the Brillouin zone the main part of the spectral weight follows the bare electron band<sup>21</sup>.

The two wave functions (10) and (19), describing respectively the small and large polaron, differentiate mainly for the expression of the phonon distribution function. It is evident that, in spite of the assumption of no correlation (sum of coherent states in the phonon coordinate), the large polaron wave function takes into account the average effect of the correlation introduced by the electron recoil (Eq.21), effect absent in the small polaron phonon distribution function.

The expectation value of the Hamiltonian (1) on the state (19) gives:

$$\begin{aligned} <\psi_{\vec{k}}^{(l)}|H_{el}|\psi_{\vec{k}}^{(l)}> &= -t \sum_{\vec{\delta}} e^{i\vec{k}\cdot\vec{\delta}} e^{-\sum_{\vec{q}}|h_{\vec{q}}|^2(1-e^{-i\vec{q}\cdot\vec{\delta}})} \left[ 1 + \sum_{\vec{q}} (h_{\vec{q}}d_{\vec{q}}^* + h.c.) (1 - e^{-i\vec{q}\cdot\vec{\delta}}) \right. \\ &\quad \left. + \sum_{\vec{q}} |d_{\vec{q}}|^2 e^{-i\vec{q}\cdot\vec{\delta}} + \sum_{\vec{q}_1} d_{\vec{q}_1} h_{\vec{q}_1}^* (e^{-i\vec{q}_1\cdot\vec{\delta}} - 1) \sum_{\vec{q}_2} d_{\vec{q}_2}^* h_{\vec{q}_2} (e^{-i\vec{q}_2\cdot\vec{\delta}} - 1) \right] \end{aligned} \quad (23)$$

$$\begin{aligned} <\psi_{\vec{k}}^{(l)}|H_{ph} + H_I|\psi_{\vec{k}}^{(l)}> &= \left[ \sum_{\vec{q}} (\omega_0|h_{\vec{q}}|^2 - M_q h_{\vec{q}}^* - M_q^* h_{\vec{q}}) \right] <\psi_{\vec{k}}^{(l)}|\psi_{\vec{k}}^{(l)}> \\ &\quad + \sum_{\vec{q}} [\omega_0|d_{\vec{q}}|^2 + (M_q - \omega_0 h_{\vec{q}}) d_{\vec{q}}^* + (M_q^* - \omega_0 h_{\vec{q}}^*) d_{\vec{q}}] \end{aligned} \quad (24)$$

where

$$<\psi_{\vec{k}}^{(l)}|\psi_{\vec{k}}^{(l)}> = 1 + \sum_{\vec{q}} |d_{\vec{q}}|^2. \quad (25)$$

Then  $d_{\vec{q}}$  is fixed by the condition:

$$\frac{\partial E_{\vec{k}}^{(l)}}{\partial d_{\vec{q}}^*} = 0. \quad (26)$$

Here  $E_{\vec{k}}^{(l)}$  is the polaron energy in the weak-coupling limit:

$$E_{\vec{k}}^{(l)} = \frac{<\psi_{\vec{k}}^{(l)}|H|\psi_{\vec{k}}^{(l)}>}{<\psi_{\vec{k}}^{(l)}|\psi_{\vec{k}}^{(l)}>}. \quad (27)$$

This procedure provides:

$$d_{\vec{q}} = \frac{M_q - \omega_0 h_{\vec{q}} - 2te^{-\sum_{\vec{q}}|h_{\vec{q}}|^2(1-\cos q_x a)} h_{\vec{q}} A_{\vec{q}}(\vec{k})}{y_{\vec{k}} - B_{\vec{k}} + 2te^{-\sum_{\vec{q}}|h_{\vec{q}}|^2(1-\cos q_x a)} \sum_{i=1}^d \cos(k_i - q_i) a} \quad (28)$$

where

$$\begin{aligned}
B_{\vec{k}} &= \omega_0 + \sum_{\vec{q}} \left[ \omega_0 |h_{\vec{q}}|^2 - M_q h_{\vec{q}}^* - M_q^* h_{\vec{q}} \right] , \\
A_{\vec{q}}(\vec{k}) &= \sum_{i=1}^d \left\{ \cos k_i a - \cos (k_i - q_i) a + x_i(\vec{k}) \left[ \cos \left( \frac{k_i}{2} - q_i \right) a - \cos \frac{k_i}{2} a \right] \right. \\
&\quad \left. + z_i(\vec{k}) \left[ \sin \left( \frac{k_i}{2} - q_i \right) a - \sin \frac{k_i}{2} a \right] \right\}
\end{aligned} \tag{29}$$

and  $x_i(\vec{k})$ ,  $z_i(\vec{k})$ ,  $y(\vec{k})$  are variational parameters.

### Intermediate coupling

For any particular value of  $t$  there is a value of the electron-phonon coupling constant ( $g_c$ ) where the ground state energies of the two previously discussed solutions become equal. Nevertheless the two solutions exhibit very different polaron features. In particular when the coupling constant is smaller than  $g_c$  the stable solution (the one with lowest energy) corresponds to the large polaron while for  $g > g_c$  it corresponds to the small polaron. Crossing  $g_c$  the mass of the polaronic quasi-particle increases in a discontinuous way<sup>14</sup>. A more careful inspection shows that in this range of  $g$  values the wave functions describing the two solutions of large and small polaron are not orthogonal and have non zero off diagonal matrix elements. This suggests that the lowest state of the system is made of a mixture of the large and small polaron solutions<sup>22</sup>. Then the idea is to use a variational method to determine the ground state energy of the hamiltonian (1) by considering as trial state a linear superposition of the wave functions describing the two types of previously discussed polarons:

$$|\psi_{\vec{k}}\rangle = \frac{A_{\vec{k}}|\overline{\psi}_{\vec{k}}^{(l)}\rangle + B_{\vec{k}}|\overline{\psi}_{\vec{k}}^{(s)}\rangle}{\sqrt{A_{\vec{k}}^2 + B_{\vec{k}}^2 + 2A_{\vec{k}}B_{\vec{k}}S_{\vec{k}}}} \tag{30}$$

where

$$|\overline{\psi}_{\vec{k}}^{(l)}\rangle = \frac{|\psi_{\vec{k}}^{(l)}\rangle}{\sqrt{\langle \psi_{\vec{k}}^{(l)} | \psi_{\vec{k}}^{(l)} \rangle}}, \quad |\overline{\psi}_{\vec{k}}^{(s)}\rangle = \frac{|\psi_{\vec{k}}^{(s)}\rangle}{\sqrt{\langle \psi_{\vec{k}}^{(s)} | \psi_{\vec{k}}^{(s)} \rangle}} \tag{31}$$

and  $S_{\vec{k}}$  is the overlap factor of the two wave functions  $|\overline{\psi}_{\vec{k}}^{(l)}\rangle$  and  $|\overline{\psi}_{\vec{k}}^{(s)}\rangle$ :

$$S_{\vec{k}} = \frac{\langle \bar{\psi}_{\vec{k}}^{(l)} | \bar{\psi}_{\vec{k}}^{(s)} \rangle + h.c.}{2}. \quad (32)$$

In the Eq.(30)  $A_{\vec{k}}$  and  $B_{\vec{k}}$  are two additional variational parameters which provide the relative weight of the large and small polaron solutions in the ground state of the system for any particular value of  $\vec{k}$ .

In this paper we perform the minimization procedure in two steps. First the energies of the large and the small polaron wave functions are minimized, then these wave functions are used in the minimization procedure discussed in the present section. This way to proceed simplifies significantly the computational effort and makes all calculations described accessible on a personal computer.

It should be noted that the trial wave function (30) contains correlation between the emission of successive virtual phonons in the field around the electron since the phonon wave function is a linear superposition of coherent states for any particular lattice site. Then the wave function (30) recovers, in the weak and strong coupling limit respectively, the large and small polaron wave function, introduces correlation between the emission of successive virtual phonons by the electron and contains the important physical information that the quasi-particle becomes unstable when the polaron excitation energy equals the energy of a longitudinal optical phonon.

The procedure of minimization of the quantity  $\frac{\langle \psi_{\vec{k}} | H | \psi_{\vec{k}} \rangle}{\langle \psi_{\vec{k}} | \psi_{\vec{k}} \rangle}$  with respect to  $A_{\vec{k}}$  and  $B_{\vec{k}}$  gives for the polaron energy:

$$E_{\vec{k}} = \frac{E_{\vec{k}m} - S_{\vec{k}} E_{\vec{k}c} - \sqrt{\left(E_{\vec{k}m} - S_{\vec{k}} E_{\vec{k}c}\right)^2 - \left(1 - S_{\vec{k}}^2\right) \left(E_{\vec{k}}^{(l)} E_{\vec{k}}^{(s)} - E_{\vec{k}c}^2\right)}}{1 - S_{\vec{k}}^2} \quad (33)$$

and

$$\frac{A_{\vec{k}}}{B_{\vec{k}}} = \frac{E_{\vec{k}c} - E_{\vec{k}} S_{\vec{k}}}{E_{\vec{k}} - E_{\vec{k}}^{(l)}}. \quad (34)$$

Here  $E_{\vec{k}m} = (E_{\vec{k}}^{(l)} + E_{\vec{k}}^{(s)})/2$  and  $E_{\vec{k}c} = \left(\langle \bar{\psi}_{\vec{k}}^{(l)} | H | \bar{\psi}_{\vec{k}}^{(s)} \rangle + h.c.\right)/2$ . Finally the overlap factor and the matrix element of the hamiltonian between the two solutions  $|\bar{\psi}_{\vec{k}}^{(l)}\rangle$  and  $|\bar{\psi}_{\vec{k}}^{(s)}\rangle$  are, respectively:

$$\begin{aligned} \langle \bar{\psi}_{\vec{k}}^{(l)} | \bar{\psi}_{\vec{k}}^{(s)} \rangle &= \sum_{\vec{R}_n} \frac{e^{i\vec{k} \cdot \vec{R}_n}}{\left( \langle \psi_{\vec{k}}^{(l)} | \psi_{\vec{k}}^{(l)} \rangle \right)^{1/2}} \frac{\phi_{\vec{k}}(-\vec{R}_n)}{\left( \langle \psi_{\vec{k}}^{(s)} | \psi_{\vec{k}}^{(s)} \rangle \right)^{1/2}} e^{-\sum_{\vec{q}} \left[ |h_{\vec{q}}|^2 + |f_{\vec{q}}|^2 - 2h_{\vec{q}}f_{\vec{q}}^* e^{-i\vec{q} \cdot \vec{R}_n} \right] / 2} \\ &\left[ 1 + \sum_{\vec{q}} d_{\vec{q}} \left( h_{\vec{q}}^* - f_{\vec{q}}^* e^{-i\vec{q} \cdot \vec{R}_n} \right) \right] \end{aligned} \quad (35)$$

and

$$\begin{aligned} \langle \bar{\psi}_{\vec{k}}^{(l)} | H_{el} | \bar{\psi}_{\vec{k}}^{(s)} \rangle &= -t \sum_{\vec{R}_n} \frac{e^{i\vec{k} \cdot \vec{R}_n}}{\left( \langle \psi_{\vec{k}}^{(l)} | \psi_{\vec{k}}^{(l)} \rangle \right)^{1/2}} \frac{e^{-\sum_{\vec{q}} \left[ |h_{\vec{q}}|^2 + |f_{\vec{q}}|^2 - 2h_{\vec{q}}f_{\vec{q}}^* e^{-i\vec{q} \cdot \vec{R}_n} \right] / 2}}{\left( \langle \psi_{\vec{k}}^{(s)} | \psi_{\vec{k}}^{(s)} \rangle \right)^{1/2}} \\ &\left[ 1 + \sum_{\vec{q}} d_{\vec{q}} \left( h_{\vec{q}}^* - f_{\vec{q}}^* e^{-i\vec{q} \cdot \vec{R}_n} \right) \right] \sum_{<\vec{\delta}>} \phi_{\vec{k}}(-\vec{R}_n - \vec{\delta}), \end{aligned} \quad (36)$$

$$\begin{aligned} \langle \bar{\psi}_{\vec{k}}^{(l)} | H_{ph} + H_I | \bar{\psi}_{\vec{k}}^{(s)} \rangle &= \sum_{\vec{R}_n} \frac{e^{i\vec{k} \cdot \vec{R}_n}}{\left( \langle \psi_{\vec{k}}^{(l)} | \psi_{\vec{k}}^{(l)} \rangle \right)^{1/2}} \frac{e^{-\sum_{\vec{q}} \left[ |h_{\vec{q}}|^2 + |f_{\vec{q}}|^2 - 2h_{\vec{q}}f_{\vec{q}}^* e^{-i\vec{q} \cdot \vec{R}_n} \right] / 2}}{\left( \langle \psi_{\vec{k}}^{(s)} | \psi_{\vec{k}}^{(s)} \rangle \right)^{1/2}} \\ &\phi_{\vec{k}}(-\vec{R}_n) \left[ \sum_{\vec{q}} d_{\vec{q}} \left( M_q^* - f_{\vec{q}}^* e^{-i\vec{q} \cdot \vec{R}_n} \right) \right. \\ &\left. + \left( 1 + \sum_{\vec{q}} d_{\vec{q}} \left( h_{\vec{q}}^* - f_{\vec{q}}^* e^{-i\vec{q} \cdot \vec{R}_n} \right) \right) \sum_{\vec{q}} \left( \omega_0 f_{\vec{q}}^* h_{\vec{q}} e^{-i\vec{q} \cdot \vec{R}_n} - M_q f_{\vec{q}}^* e^{-i\vec{q} \cdot \vec{R}_n} - M_q^* h_{\vec{q}} \right) \right]. \end{aligned} \quad (37)$$

### III. NUMERICAL RESULTS

In order to test the validity of our variational approach we recall the perturbative results both in the weak and strong coupling limits. From the weak coupling perturbative theory we get<sup>6</sup>:

$$E_{\vec{k}}^{(wc)} = E_b(\vec{k}) + \Re \left[ \Sigma(\vec{k}, E_b(\vec{k})) \right] \quad (38)$$

where

$$\Sigma(\vec{k}, ik_n) = \sum_{\vec{q}} \frac{|M_q|^2}{ik_n - \omega_0 - E_b(\vec{k} + \vec{q})} \quad (39)$$

while the second order perturbation theory in the strong coupling limit gives<sup>7</sup>:

$$E_{\vec{k}}^{(sc)} \simeq E_p \left( 1 + \frac{1}{4\lambda^2} \right) - 2te^{-g^2} \cos k_x - 2 \frac{E_p}{4\lambda^2} e^{-g^2} \cos 2k_x \quad (40)$$

in one dimension and

$$\begin{aligned} E_{\vec{k}}^{(sc)} \simeq & E_p \left( 1 + \frac{1}{8\lambda^2} \right) - 2te^{-g^2} (\cos k_x + \cos k_y) \\ & - 2\frac{E_p}{8\lambda^2} e^{-g^2} (\cos 2k_x + \cos 2k_y + 2 \cos k_x \cos k_y) \end{aligned} \quad (41)$$

in two dimensions.

In Fig.1. and Fig.2. we report the polaron ground state energy obtained within our approach ( $E_{\vec{k}=0}$  in the Eq.(33)) in one and two dimensions together with large and small polaron estimates (Eq.(27) and Eq.(46)), on which our solution is based, and with the perturbative results. As it is clear from the plots, our variational proposal recovers the asymptotic perturbative results and improves significantly both variational estimates in the intermediate region, where neither the perturbative methods nor the asymptotic variational ansatz give a satisfactory description. Moreover, our data in the intermediate region are in very good agreement with the results of two of the best methods available in the literature (see Fig.3.): the Global Local variational method<sup>13</sup> and the Quantum Monte Carlo calculation<sup>9</sup>. The agreement of our results with approaches numerically much more sophisticated indicates that the true wave function is very close to a superposition of the wave functions that we have classified as large and small polaron solutions. The very accurate choice of the variational wave function has allowed a dramatic simplification of the numerical problem.

Within our approach we have also studied the polaron band both in one and two dimensions for different values of the electron-phonon coupling constant (Fig.4. and Fig.5.). As for the ground state energy our variational ansatz is able to recover all the properties expected. In the weak coupling regime, increasing the value of the wavenumber of the polaron Bloch state,  $E_{\vec{k}}$  increases until the excitation energy  $E_{\vec{k}} - E_{\vec{k}=0}$  equals  $\omega_0$ . When  $k$  is greater than this critical momentum the polaron becomes unstable to optical phonon emission and the dispersion curve bends over and becomes horizontal (this does not happen for  $t/\omega_0 < .25$  in one dimension and  $t/\omega_0 < .125$  in two dimensions). In the opposite regime the well-known polaronic band collapse takes place. Finally for intermediate values of the electron-phonon coupling constant the polaron band structure deviates significantly from both the dispersion

curves. In particular the strong coupling variational result underestimates the bandwidth and overestimates significantly the mass enhancement.

From our results and in agreement with Romero et al.<sup>13</sup> we find that there is not qualitative difference between the polaron features in one and two dimensions. In both cases, also in the adiabatic regime, there is a range of intermediate values of the electron-phonon coupling constant where a crossover takes place between the weak coupling regime, characterized by effective masses lightly heavier than the free electron mass, and the strong coupling regime in which the well known polaronic band collapse takes place.

Another property of interest in studying the polaronic properties is the ground state spectral weight:

$$Z_{\vec{k}} = | \langle \psi_{\vec{k}} | c_k^\dagger | 0 \rangle |^2 \quad (42)$$

where  $|0\rangle$  is the electronic vacuum state containing no phonons.  $Z_{\vec{k}}$  is the renormalization coefficient of the one-electron Green function and gives the fraction of the bare electron state in the polaronic trial wave function. In Fig.6. and Fig.7. we report the numerical results of  $Z_{\vec{k}}$ , at  $\omega_0/t = 1$ , as a function of the electron-phonon coupling constant at  $k = 0$  and as a function of the polaron Bloch state wavenumber for different values of  $g$ . In the weak coupling regime  $Z_{\vec{k}=0}$  is of order of the unity indicating that the polaronic quasi-particle is well-defined. The main part of the spectral weight is located at energies that correspond approximatively to the bare electronic levels. Instead at the edges of the Brillouin zone  $Z_{\vec{k}}$  approaches zero. For these values of the wavenumber of the polaron Bloch state the main part of the spectral weight follows the bare electron band. Increasing the electron-phonon interaction  $Z_{\vec{k}=0}$  decreases and approaches zero in the strong coupling regime. Here the carrier acquires large effective mass, the mean number of phonons in the cloud around the electron is very large and the most of spectral weight is located at the excited states, indicating that the coherent motion is suppressed rapidly with increasing the temperature<sup>23</sup>.

Finally we consider the lattice displacement associated to the polaron formation. An estimate of the average deviation of the diatomic molecule on the site  $n + m$  from the

equilibrium position, when one electron is on the site  $n$ , is given by the function:

$$D_{\vec{k}}(\vec{R}_m) = 2g \frac{S_{\vec{k}}(\vec{R}_m)}{\sqrt{2M\omega_0}} \quad (43)$$

where

$$S_{\vec{k}}(\vec{R}_m) = \frac{\sum_{\vec{R}_n} \Gamma_{\vec{k}}(\vec{R}_n, \vec{R}_m)}{2g} . \quad (44)$$

Here  $M$  denotes the ionic mass and  $\Gamma_{\vec{k}}(\vec{R}_n, \vec{R}_m)$  represents the correlation function between the electronic density on the site  $n$  and the ionic displacement on the site  $n + m$ :

$$\Gamma_{\vec{k}}(\vec{R}_n, \vec{R}_m) = \langle \psi_{\vec{k}} | c_n^\dagger c_n (a_{n+m} + a_{n+m}) | \psi_{\vec{k}} \rangle . \quad (45)$$

In Fig.8. we report the numerical results of the dimensionless quantity  $S_{\vec{k}}(\vec{R}_m)$ , at  $\omega_0/t = 0.5$  and in one dimension, for different values of the electron-phonon coupling constant at  $\vec{k} = 0$ . In the weak-coupling regime  $S_{\vec{k}=0}(\vec{R}_m)$  decreases very slowly with increasing the value of  $m$ . This is consistent with the assertion that in this regime the extension of the polaron is large compared with the lattice parameter of the crystal. In the strong coupling regime  $S_{\vec{k}=0}(\vec{R}_m)$  is different from zero only for  $\vec{R}_m = 0$ , i.e. the lattice displacement is different from zero only on the cell where there is the electron, indicating that the quasi-particle are extremely localized. Furthermore the crossover from large to small polaron is very smooth.

#### IV. CONCLUSIONS

In this paper a new variational approach has been developed to investigate the polaron features of the Holstein molecular crystal model. It has been found that a simple linear superposition of Bloch states that describe the small and large polaron solutions provides an estimate of the ground state energy that is in very good agreement with the best results available. It has been possible to identify a range of intermediate values of the electron-phonon coupling constant where a crossover takes place between the weak and strong coupling regime. Here the small and large polaron wave functions are not orthogonal and both

contribute to the formation of the so called intermediate polaron. We stress that the new variational approach does not require any significant computational effort to be implemented and involves, for any particular  $k$  value, a very small number of variational parameters, that does not depend on the number of lattice sites.

## V. APPENDIX

In the Holstein model ( $M_q = \omega_0 g / \sqrt{N}$ ) the standard trigonometric integrals in the Eq.(13), Eq.(14) and Eq.(15) can be performed analytically. In one dimension the polaron energy in the strong coupling limit assumes the following form ( $a = \omega_0 = 1$ ):

$$E_{\vec{k}}^{(s)} = \frac{\langle \psi_{\vec{k}}^{(s)} | H | \psi_{\vec{k}}^{(s)} \rangle}{\langle \psi_{\vec{k}}^{(s)} | \psi_{\vec{k}}^{(s)} \rangle} \quad (46)$$

where

$$\begin{aligned} \langle \psi_{\vec{k}}^{(s)} | \psi_{\vec{k}}^{(s)} \rangle &= 1 + 2 \cos k_x (2\alpha_{\vec{k}}\beta_{\vec{k}} + 2\beta_{\vec{k}}\gamma_{\vec{k}}) e^{-g^2(\alpha_{\vec{k}}^4 + 2\beta_{\vec{k}}^4 + 2\gamma_{\vec{k}}^4 - 2\alpha_{\vec{k}}^2\beta_{\vec{k}}^2 - 2\beta_{\vec{k}}^2\gamma_{\vec{k}}^2)} \\ &+ 2 \cos 2k_x (\beta_{\vec{k}}^2 + 2\gamma_{\vec{k}}\alpha_{\vec{k}}) e^{-g^2(\alpha_{\vec{k}}^4 + \beta_{\vec{k}}^4 + 2\gamma_{\vec{k}}^4 - 2\gamma_{\vec{k}}^2\alpha_{\vec{k}}^2)} + 4 \cos 3k_x \beta_{\vec{k}}\gamma_{\vec{k}} e^{-g^2(\alpha_{\vec{k}}^4 + 2\beta_{\vec{k}}^4 + 2\gamma_{\vec{k}}^4 - 2\gamma_{\vec{k}}^2\beta_{\vec{k}}^2)} \\ &+ 2 \cos 4k_x \gamma_{\vec{k}}^2 e^{-g^2(\alpha_{\vec{k}}^4 + 2\beta_{\vec{k}}^4 + \gamma_{\vec{k}}^4)}, \end{aligned} \quad (47)$$

$$\begin{aligned} \langle \psi_{\vec{k}}^{(s)} | H_{el} | \psi_{\vec{k}}^{(s)} \rangle &= -t (4\alpha_{\vec{k}}\beta_{\vec{k}} + 4\beta_{\vec{k}}\gamma_{\vec{k}}) \\ &- 2t \cos k_x (2\alpha_{\vec{k}}\gamma_{\vec{k}} + \beta_{\vec{k}}^2 + 1) e^{-g^2(\alpha_{\vec{k}}^4 + 2\beta_{\vec{k}}^4 + 2\gamma_{\vec{k}}^4 - 2\alpha_{\vec{k}}^2\beta_{\vec{k}}^2 - 2\beta_{\vec{k}}^2\gamma_{\vec{k}}^2)} \\ &- 2t \cos 2k_x (4\beta_{\vec{k}}\gamma_{\vec{k}} + 2\beta_{\vec{k}}\alpha_{\vec{k}}) e^{-g^2(\alpha_{\vec{k}}^4 + \beta_{\vec{k}}^4 + 2\gamma_{\vec{k}}^4 - 2\gamma_{\vec{k}}^2\alpha_{\vec{k}}^2)} \\ &- 2t \cos 3k_x (2\alpha_{\vec{k}}\gamma_{\vec{k}} + \beta_{\vec{k}}^2 + \gamma_{\vec{k}}^2) e^{-g^2(\alpha_{\vec{k}}^4 + 2\beta_{\vec{k}}^4 + 2\gamma_{\vec{k}}^4 - 2\gamma_{\vec{k}}^2\beta_{\vec{k}}^2)} \\ &- 4t \cos 4k_x \gamma_{\vec{k}}\beta_{\vec{k}} e^{-g^2(\alpha_{\vec{k}}^4 + 2\beta_{\vec{k}}^4 + \gamma_{\vec{k}}^4)} - 2t \cos 5k_x \gamma_{\vec{k}}^2 e^{-g^2(\alpha_{\vec{k}}^4 + 2\beta_{\vec{k}}^4 + 2\gamma_{\vec{k}}^4)} \end{aligned} \quad (48)$$

and

$$\begin{aligned} \langle \psi_{\vec{k}}^{(s)} | H_{ph} + H_I | \psi_{\vec{k}}^{(s)} \rangle &= -g^2 (\alpha_{\vec{k}}^4 + 2\beta_{\vec{k}}^4 + 2\gamma_{\vec{k}}^4) \\ &+ g^2 [(2\alpha_{\vec{k}}\beta_{\vec{k}} + 2\beta_{\vec{k}}\gamma_{\vec{k}}) (2\alpha_{\vec{k}}^2\beta_{\vec{k}}^2 + 2\beta_{\vec{k}}^2\gamma_{\vec{k}}^2) - 2\alpha_{\vec{k}}^3\beta_{\vec{k}} - 2\beta_{\vec{k}}^3\gamma_{\vec{k}} - 2\beta_{\vec{k}}^3\alpha_{\vec{k}} - 2\gamma_{\vec{k}}^3\beta_{\vec{k}}] \end{aligned}$$

$$\begin{aligned}
& 2 \cos k_x e^{-g^2 \left( \alpha_{\vec{k}}^4 + 2\beta_{\vec{k}}^4 + 2\gamma_{\vec{k}}^4 - 2\alpha_{\vec{k}}^2\beta_{\vec{k}}^2 - 2\beta_{\vec{k}}^2\gamma_{\vec{k}}^2 \right)} \\
& + g^2 \left[ \left( \beta_{\vec{k}}^2 + 2\gamma_{\vec{k}}\alpha_{\vec{k}} \right) \left( \beta_{\vec{k}}^4 + 2\gamma_{\vec{k}}^2\alpha_{\vec{k}}^2 \right) - 2\beta_{\vec{k}}^4 - 2\gamma_{\vec{k}}^3\alpha_{\vec{k}} - 2\gamma_{\vec{k}}\alpha_{\vec{k}}^3 \right] 2 \cos 2k_x e^{-g^2 \left( \alpha_{\vec{k}}^4 + \beta_{\vec{k}}^4 + 2\gamma_{\vec{k}}^4 - 2\gamma_{\vec{k}}^2\alpha_{\vec{k}}^2 \right)} \\
& + g^2 \left( 4\beta_{\vec{k}}^3\gamma_{\vec{k}}^3 - 2\gamma_{\vec{k}}\beta_{\vec{k}}^3 - 2\gamma_{\vec{k}}^3\beta_{\vec{k}} \right) 2 \cos 3k_x e^{-g^2 \left( \alpha_{\vec{k}}^4 + 2\beta_{\vec{k}}^4 + 2\gamma_{\vec{k}}^4 - 2\gamma_{\vec{k}}^2\beta_{\vec{k}}^2 \right)} \\
& + g^2 \left( \gamma_{\vec{k}}^6 - 2\gamma_{\vec{k}}^4 \right) 2 \cos 4k_x e^{-g^2 \left( \alpha_{\vec{k}}^4 + 2\beta_{\vec{k}}^4 + \gamma_{\vec{k}}^4 \right)}. \tag{49}
\end{aligned}$$

In two dimensions we have

$$\begin{aligned}
& \langle \psi_{\vec{k}}^{(s)} | \psi_{\vec{k}}^{(s)} \rangle = 1 + (\cos k_x + \cos k_y) \left( 4\alpha_{\vec{k}}\beta_{\vec{k}} + 8\beta_{\vec{k}}\gamma_{\vec{k}} \right) e^{-g^2 \left( \alpha_{\vec{k}}^4 + 4\beta_{\vec{k}}^4 + 4\gamma_{\vec{k}}^4 - 2\alpha_{\vec{k}}^2\beta_{\vec{k}}^2 - 4\beta_{\vec{k}}^2\gamma_{\vec{k}}^2 \right)} \\
& + (\cos 2k_x + \cos 2k_y) \left( 2\beta_{\vec{k}}^2 + 4\gamma_{\vec{k}}^2 \right) e^{-g^2 \left( \alpha_{\vec{k}}^4 + 3\beta_{\vec{k}}^4 + 2\gamma_{\vec{k}}^4 \right)} \\
& + \cos k_x \cos k_y \left( 8\alpha_{\vec{k}}\gamma_{\vec{k}} + 8\beta_{\vec{k}}^2 \right) e^{-g^2 \left( \alpha_{\vec{k}}^4 + 2\beta_{\vec{k}}^4 + 4\gamma_{\vec{k}}^4 - 2\gamma_{\vec{k}}^2\alpha_{\vec{k}}^2 \right)} \\
& + (\cos 2k_x \cos k_y + \cos 2k_y \cos k_x) 8\beta_{\vec{k}}\gamma_{\vec{k}} e^{-g^2 \left( \alpha_{\vec{k}}^4 + 4\beta_{\vec{k}}^4 + 4\gamma_{\vec{k}}^4 - 2\gamma_{\vec{k}}^2\beta_{\vec{k}}^2 \right)} \\
& + \cos 2k_x \cos 2k_y 4\gamma_{\vec{k}}^2 e^{-g^2 \left( \alpha_{\vec{k}}^4 + 4\beta_{\vec{k}}^4 + 3\gamma_{\vec{k}}^4 \right)}, \tag{50}
\end{aligned}$$

$$\begin{aligned}
& \langle \psi_{\vec{k}}^{(s)} | H_{el} | \psi_{\vec{k}}^{(s)} \rangle = -t \left( 8\alpha_{\vec{k}}\beta_{\vec{k}} + 16\beta_{\vec{k}}\gamma_{\vec{k}} \right) \\
& - t (\cos k_x + \cos k_y) \left( 10\beta_{\vec{k}}^2 + 4\gamma_{\vec{k}}^2 + 2 + 8\alpha_{\vec{k}}\gamma_{\vec{k}} \right) e^{-g^2 \left( \alpha_{\vec{k}}^4 + 4\beta_{\vec{k}}^4 + 4\gamma_{\vec{k}}^4 - 2\alpha_{\vec{k}}^2\beta_{\vec{k}}^2 - 4\beta_{\vec{k}}^2\gamma_{\vec{k}}^2 \right)} \\
& - t (\cos 2k_x + \cos 2k_y) \left( 4\alpha_{\vec{k}}\beta_{\vec{k}} + 16\beta_{\vec{k}}\gamma_{\vec{k}} \right) e^{-g^2 \left( \alpha_{\vec{k}}^4 + 3\beta_{\vec{k}}^4 + 2\gamma_{\vec{k}}^4 \right)} \\
& - t (\cos 3k_x + \cos 3k_y) \left( 2\beta_{\vec{k}}^2 + 4\gamma_{\vec{k}}^2 \right) e^{-g^2 \left( \alpha_{\vec{k}}^4 + 4\beta_{\vec{k}}^4 + 4\gamma_{\vec{k}}^4 \right)} \\
& - t \cos k_x \cos k_y \left( 16\beta_{\vec{k}}\alpha_{\vec{k}} + 48\gamma_{\vec{k}}\beta_{\vec{k}} \right) e^{-g^2 \left( \alpha_{\vec{k}}^4 + 2\beta_{\vec{k}}^4 + 4\gamma_{\vec{k}}^4 - 2\alpha_{\vec{k}}^2\gamma_{\vec{k}}^2 \right)} \\
& - t (\cos 2k_x \cos k_y + \cos 2k_y \cos k_x) \left( 12\beta_{\vec{k}}^2 + 12\gamma_{\vec{k}}^2 + 8\alpha_{\vec{k}}\gamma_{\vec{k}} \right) e^{-g^2 \left( \alpha_{\vec{k}}^4 + 4\beta_{\vec{k}}^4 + 4\gamma_{\vec{k}}^4 - 2\beta_{\vec{k}}^2\gamma_{\vec{k}}^2 \right)} \\
& - t \cos 2k_x \cos 2k_y 16\beta_{\vec{k}}\gamma_{\vec{k}} e^{-g^2 \left( \alpha_{\vec{k}}^4 + 4\beta_{\vec{k}}^4 + 3\gamma_{\vec{k}}^4 \right)} \\
& - t (\cos 3k_x \cos k_y + \cos 3k_y \cos k_x) 8\beta_{\vec{k}}\gamma_{\vec{k}} e^{-g^2 \left( \alpha_{\vec{k}}^4 + 4\beta_{\vec{k}}^4 + 4\gamma_{\vec{k}}^4 \right)} \\
& - t (\cos 3k_x \cos 2k_y + \cos 3k_y \cos 2k_x) 4\gamma_{\vec{k}}^2 e^{-g^2 \left( \alpha_{\vec{k}}^4 + 4\beta_{\vec{k}}^4 + 4\gamma_{\vec{k}}^4 \right)} \tag{51}
\end{aligned}$$

and

$$\begin{aligned}
& \langle \psi_{\vec{k}}^{(s)} | H_{ph} + H_I | \psi_{\vec{k}}^{(s)} \rangle = -g^2 \left( \alpha_{\vec{k}}^4 + 4\beta_{\vec{k}}^4 + 4\gamma_{\vec{k}}^4 \right) \\
& + g^2 \left[ \left( 4\alpha_{\vec{k}}\beta_{\vec{k}} + 8\beta_{\vec{k}}\gamma_{\vec{k}} \right) \left( 2\alpha_{\vec{k}}^2\beta_{\vec{k}}^2 + 4\beta_{\vec{k}}^2\gamma_{\vec{k}}^2 \right) - 4\alpha_{\vec{k}}^3\beta_{\vec{k}} - 8\beta_{\vec{k}}^3\gamma_{\vec{k}} - 4\beta_{\vec{k}}^3\alpha_{\vec{k}} - 8\gamma_{\vec{k}}^3\beta_{\vec{k}} \right]
\end{aligned}$$

$$\begin{aligned}
& (\cos k_x + \cos k_y) e^{-g^2 \left( \alpha_{\vec{k}}^4 + 4\beta_{\vec{k}}^4 + 4\gamma_{\vec{k}}^4 - 2\alpha_{\vec{k}}^2\beta_{\vec{k}}^2 - 4\beta_{\vec{k}}^2\gamma_{\vec{k}}^2 \right)} \\
& + g^2 \left[ (2\beta_{\vec{k}}^2 + 4\gamma_{\vec{k}}^2) (2\beta_{\vec{k}}^4 + 2\gamma_{\vec{k}}^4) - 4\beta_{\vec{k}}^4 - 8\gamma_{\vec{k}}^4 \right] (\cos 2k_x + \cos 2k_y) e^{-g^2 \left( \alpha_{\vec{k}}^4 + 3\beta_{\vec{k}}^4 + 2\gamma_{\vec{k}}^4 \right)} \\
& + g^2 \left[ (8\alpha_{\vec{k}}\gamma_{\vec{k}} + 8\beta_{\vec{k}}^2) (2\beta_{\vec{k}}^4 + 2\gamma_{\vec{k}}^2\alpha_{\vec{k}}^2) - 8\alpha_{\vec{k}}^3\gamma_{\vec{k}} - 16\beta_{\vec{k}}^4 - 8\alpha_{\vec{k}}\gamma_{\vec{k}}^3 \right] \\
& \cos k_x \cos k_y e^{-g^2 \left( \alpha_{\vec{k}}^4 + 2\beta_{\vec{k}}^4 + 4\gamma_{\vec{k}}^4 - 2\gamma_{\vec{k}}^2\alpha_{\vec{k}}^2 \right)} \\
& + g^2 \left( 16\beta_{\vec{k}}^3\gamma_{\vec{k}}^3 - 8\beta_{\vec{k}}^3\gamma_{\vec{k}} - 8\beta_{\vec{k}}\gamma_{\vec{k}}^3 \right) (\cos 2k_x \cos k_y + \cos 2k_y \cos k_x) e^{-g^2 \left( \alpha_{\vec{k}}^4 + 4\beta_{\vec{k}}^4 + 4\gamma_{\vec{k}}^4 - 2\gamma_{\vec{k}}^2\beta_{\vec{k}}^2 \right)} \\
& + g^2 \left[ 4\gamma_{\vec{k}}^6 - 8\gamma_{\vec{k}}^4 \right] \cos 2k_x \cos 2k_y e^{-g^2 \left( \alpha_{\vec{k}}^4 + 4\beta_{\vec{k}}^4 + 3\gamma_{\vec{k}}^4 \right)}. \tag{52}
\end{aligned}$$


---

<sup>1</sup> J.P. Falk, M. A. Kastner, and R. J. Birgenau, Phys. Rev. B **48**, 4043 (1993); Xiang-Xin Bi and Peter C. Eklund, Phys. Rev. Lett. **70**, 2625 (1993); K. H. Kim, J. H. Jung, and T. W. Noh, cond-mat/9804167 (1998); P. Calvani, Proceedings of the *International School of Physics Enrico Fermi*, Course CXXXVI, Varenna (1997).

<sup>2</sup> Guo-meng-Zhao, K. Conder, H. Keller, and K. A. Muller, Nature **381**, 676 (1996); Guo-Meng-Zhao, M. B. Hunt, H. Keller, and K. A. Muller, Nature **385**, 236 (1997); K. H. Kim, J. Y. Gu, H. S. Choi, G. W. Park, and T. W. Noh, Phys. Rev. Lett. **77**, 1877 (1996); S. J. L. Billinge, R. G. Di Francesco, G. H. Kwei, J. J. Neumeier, and J. D. Thompson, Phys. Rev. Lett. **77**, 715 (1996); A. J. Millis, P. B. Littlewood, and B. I. Shraiman, Phys. Rev. Lett. **74**, 5144 (1995); J. M. De Teresa, M. R. Ibarra, P. A. Algarabel, C. Ritter, C. Marquina, J. Blasco, J. Garcia, A. del Moral and Z. Arnold, Nature **386**, 256 (1997); J. B. Goodenough and J. S. Zhou, Nature **386**, 229 (1997); J. S. Zhou, W. Archibald, and J. B. Goodenough, Nature **381**, 770 (1996).

<sup>3</sup> A. Lanzara, N. L. Saini, M. Brunelli, F. Natali, A. Bianconi, P. G. Radaelli, S. W. Cheong, Phys. Rev. Lett. **81**, 878 (1998).

<sup>4</sup> A. Bianconi, N. L. Saini, A. Lanzara, M. Missori, T. Rossetti, H. Oyanagi, H. Yamaguchi, K. Oka and T. Ito, Phys. Rev. Lett. **76**, 3412 (1996).

<sup>5</sup> T. Holstein, Ann. Phys. **8**, 325 (1959) and **8**, 343 (1959); D. Emin, Adv. Phys. **22**, 57 (1973); for recent reviews on the polarons, see A. S. Alexandrov and N. F. Mott, Rep. Prog. Phys. **57**, 1197 (1994).

<sup>6</sup> A. B. Migdal, Sov. Phys. JETP **7**, 996 (1958).

<sup>7</sup> F. Marsiglio, Physica C **244**, 21 (1995); I. J. Lang and Yu. A. Firsov, Soviet Physics JETP **16**, 1301 (1963); Yu. A. Firsov, Polarons (Moscow, Nauka, 1975); A. A. Gogolin, Phys. Status Solidi **109**, 95 (1982); W. Stephan, Phys. Rev. B **54**, 8981 (1996).

<sup>8</sup> H. de Raedt and Ad Lagendijk, Phys. Rev. B **27**, 6097 (1983) and Phys. Rev. B **30**, 1671 (1984).

<sup>9</sup> P. E. Kornilovitch, Phys. Rev. Lett. **81**, 5382 (1998).

<sup>10</sup> J. Ranninger and U. Thibblin, Phys. Rev. B **45**, 7730 (1992); E. de Mello and J. Ranninger, Phys. Rev. B **55**, 14872 (1997); A. Kongeter and M. Wagner, J. Chem. Phys. **92**, 4003 (1990); M. Capone, W. Stephan, and M. Grilli, Phys. Rev. B **56**, 4484 (1997); A. S. Alexandrov, V. V. Kabanov and D. K. Ray, Phys. Rev. B **49**, 9915 (1994); G. Wellein and H. Fehske, Phys. Rev. B **56**, 4513 (1997); H. Fehske, J. Loos, and G. Wellein, Z. Phys. B **104**, 619 (1997).

<sup>11</sup> S. Ciuchi, F. de Pasquale, S. Fratini, and D. Feinberg, Phys. Rev. B **56**, 4494 (1997); S. Ciuchi, F. de Pasquale, and D. Feinberg, Physica C **235-240**, 2389 (1994).

<sup>12</sup> S. R. White, Phys. Rev. B **48**, 10345 (1993); E. Jeckelmann and S. R. White, Phys. Rev. B **57**, 6376 (1998).

<sup>13</sup> A. H. Romero, D. W. Brown, and K. Lindenberg, Phys. Rev. B **59**, 13728 (1999); J. Comp. Phys. **109**, 6540 (1998); cond-mat/9809025 (1998) and cond-mat/9710321 (1998).

<sup>14</sup> G. Iadonisi, V. Cataudella and D. Ninno Phys. Sta. Sol. (b) **203**, 411 (1997); G. Iadonisi, V. Cataudella, G. De Filippis, and D. Ninno, Europhys. Lett. **41**, 309 (1998); Y. Lepine and Y. Frongillo, Phys. Rev. B **46**, 14510 (1992).

<sup>15</sup> H. Lowen, Phys. Rev. B **37**, 8661 (1988); B. Gerlach and H. Lowen, Rev. Mod. Phys. **63**, 63

(1991).

<sup>16</sup> S. I. Pekar, Zh. Eksp. Teor. Fiz. **16**, 335 (1946); Ad Lagendijk and H. de Raedt, Phys. Lett. **108A**, 91 (1985). In these two references the adiabatic approximation is developed within the Frohlich and Holstein model respectively.

<sup>17</sup> Y. Toyozawa, Prog. Theor. Phys. **26**, 29 (1961).

<sup>18</sup> H. Frohlich, H. Pelzer, and S. Zienau, Philos. Mag. **41**, 221 (1950); H. Frohlich, in *Polarons and Excitons*, C. G. Kuper and G. A. Whitfield Eds. (Oliver and Boyd, Edinburg, 1963) pag. 1.

<sup>19</sup> T.D. Lee, F. Low, and D. Pines, Phys. Rev. **90**, 297 (1953).

<sup>20</sup> E. Haga, Progr. Theoret. Phys. **13**, 555 (1955); D. M. Larsen, Phys. Rev. **144**, 697 (1966).

<sup>21</sup> S. Engelsberg and J. R. Schrieffer, Phys. Rev. B **131**, 993 (1963).

<sup>22</sup> D. M. Eagles, Phys. Rev. **145**, 645 (1966); D. M. Eagles, J. Phys. C **17**, 637 (1984); D. M. Eagles, Phys. Rev. **181**, 1278 (1969).

<sup>23</sup> D. Emin, Phys. Rev. B **48**, 13691 (1993).

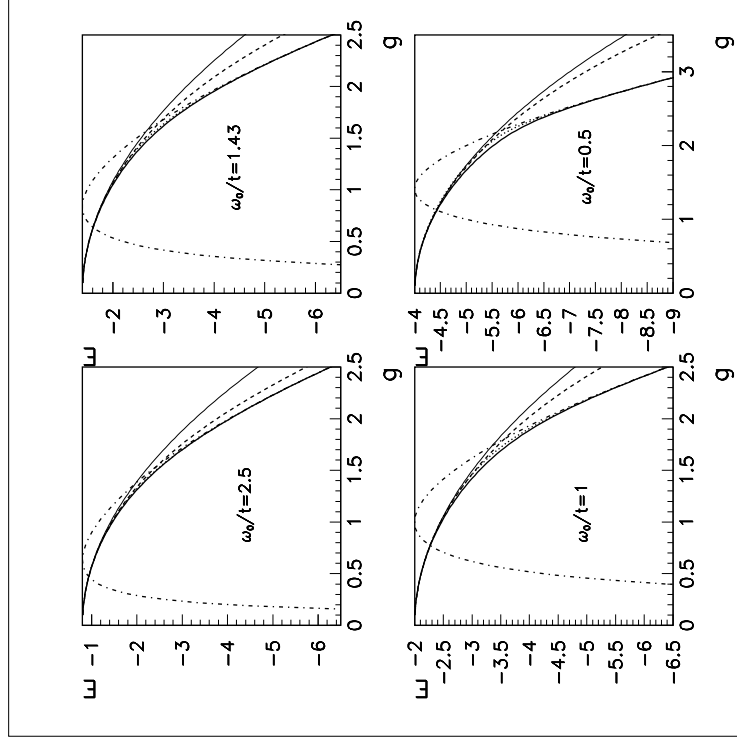


FIG. 1. The polaron ground state energy ( $E_{\vec{k}=0}$  in the Eq.(33)) in one dimension (thick solid line) is reported as a function of the electron-phonon coupling constant for different values of the adiabatic parameter  $\omega_0/t$ . The data obtained within the approach discussed in this paper are compared with the results of strong  $E^{(sc)}$  (Eq.(17), dashed-dotted line) and weak coupling perturbation theory  $E_{\vec{k}=0}^{(wc)}$  (Eq.(38), thin solid line) and strong (dotted line) and the weak (dashed line) coupling variational estimates  $E_{\vec{k}}^{(s)}$  (Eq.(46)) and  $E_{\vec{k}}^{(l)}$  (Eq.(27)). The energies are given in units of  $\omega_0$ .

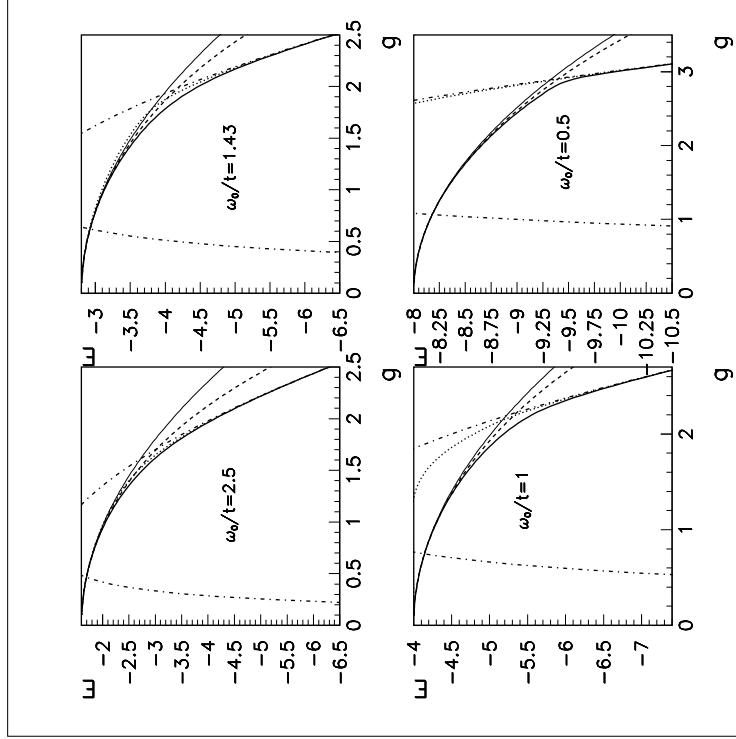


FIG. 2. The polaron ground state energy ( $E_{\vec{k}=0}$  in the Eq.(33)) in two dimensions (thick solid line) is reported as a function of the electron-phonon coupling constant for different values of the adiabatic parameter  $\omega_0/t$ . The data obtained within the approach discussed in this paper are compared with the results of strong  $E^{(sc)}$  (Eq.(17), dotted-dashed line) and weak coupling perturbation theory  $E_{\vec{k}=0}^{(wc)}$  (Eq.(38), thin solid line) and strong (dotted) and the weak (dashed line) coupling variational estimates  $E_{\vec{k}}^{(s)}$  (Eq.(46)) and  $E_{\vec{k}}^{(l)}$  (Eq.(27)). The energies are given in units of  $\omega_0$ .

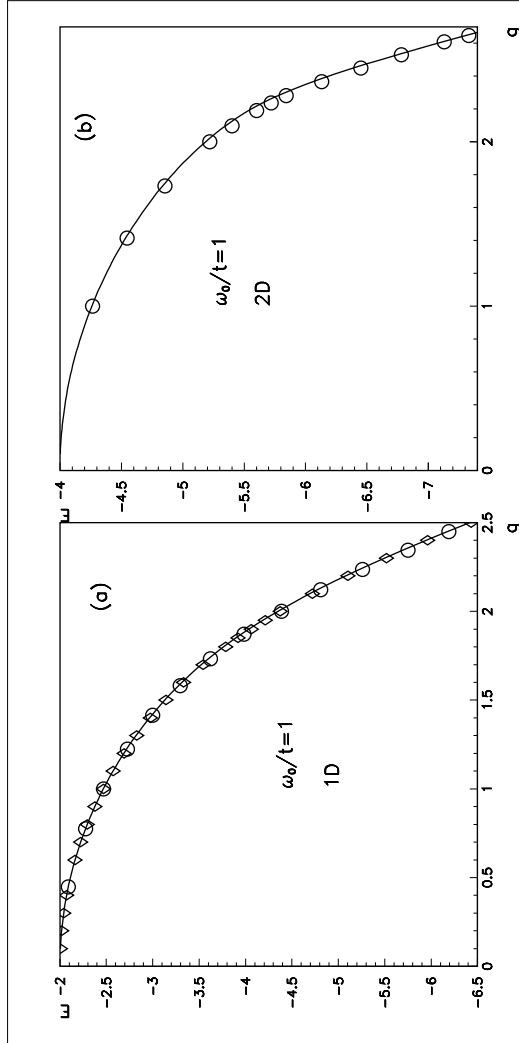


FIG. 3. The variational results obtained within the approach discussed in this paper (Eq.(33), solid line) are compared with the data of the Global Local variational method<sup>13</sup> (diamonds), kindly provided by A. H. Romero, in one dimensions (Fig.3a.) and with the energies calculated with a Quantum Monte Carlo algorithm<sup>9</sup> (circles), kindly provided by P. E. Kornilovitch, in one and two dimensions (Fig.3a. and Fig.3b.) at  $\omega_0/t = 1$ . The energies are given in units of  $\omega_0$ .

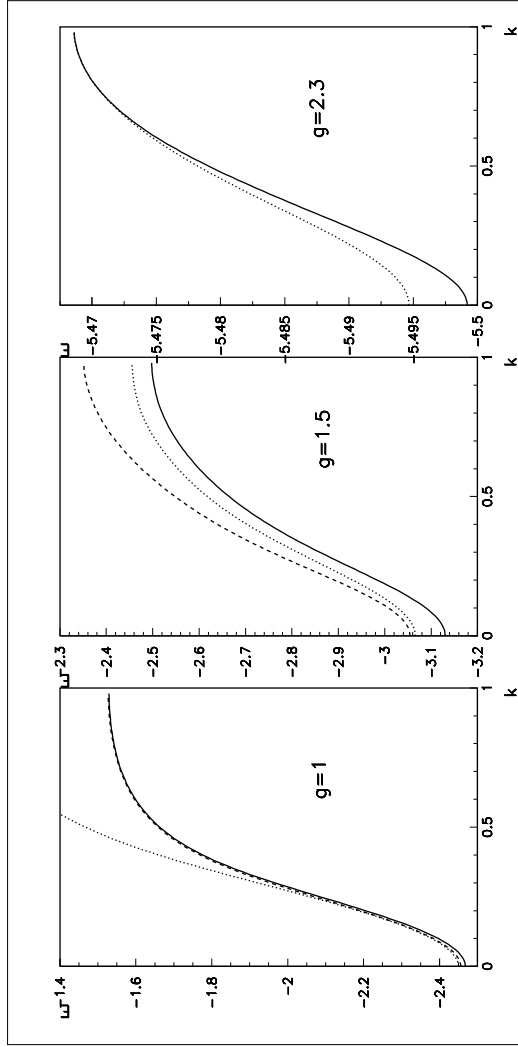


FIG. 4. The polaron band structure (solid line) in one dimension at  $\omega_0/t = 1$  is reported for different values of the electron-phonon coupling constant and it is compared with the weak (dashed line) and strong (dotted line) coupling variational estimates,  $E_{\vec{k}}^{(l)}$  and  $E_{\vec{k}}^{(s)}$ . The energies and the momenta are given in units of  $\omega_0$  and  $\pi/a$  respectively.

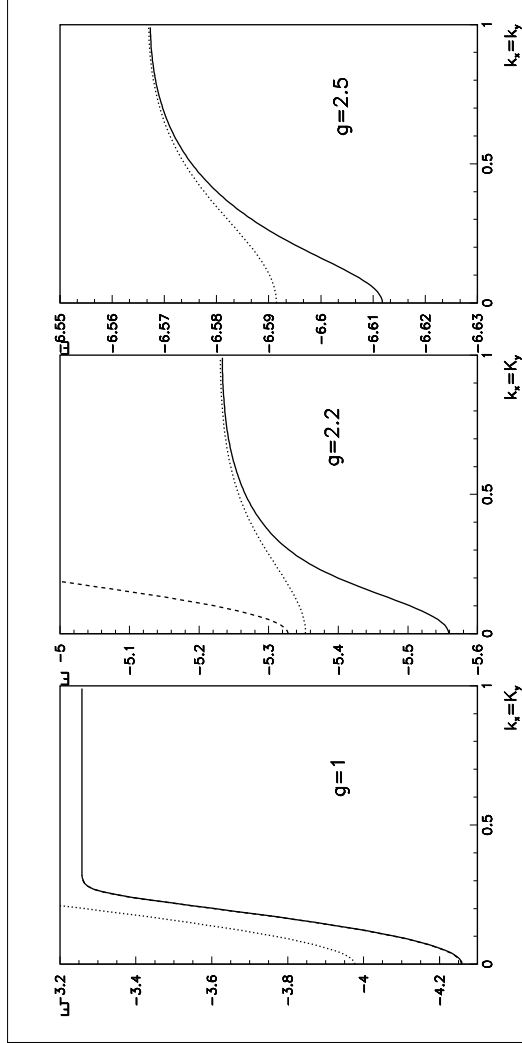


FIG. 5. The polaron band structure along the diagonal ( $k_x = k_y$ ) of the lattice in two dimensions at  $\omega_0/t = 1$  is reported for different values of the electron-phonon coupling constant and it is compared with the weak (dashed line) and strong (dotted line) coupling variational estimates,  $E_{\vec{k}}^{(l)}$  and  $E_{\vec{k}}^{(s)}$ . The energies and the momenta are given in units of  $\omega_0$  and  $\pi/a$  respectively.

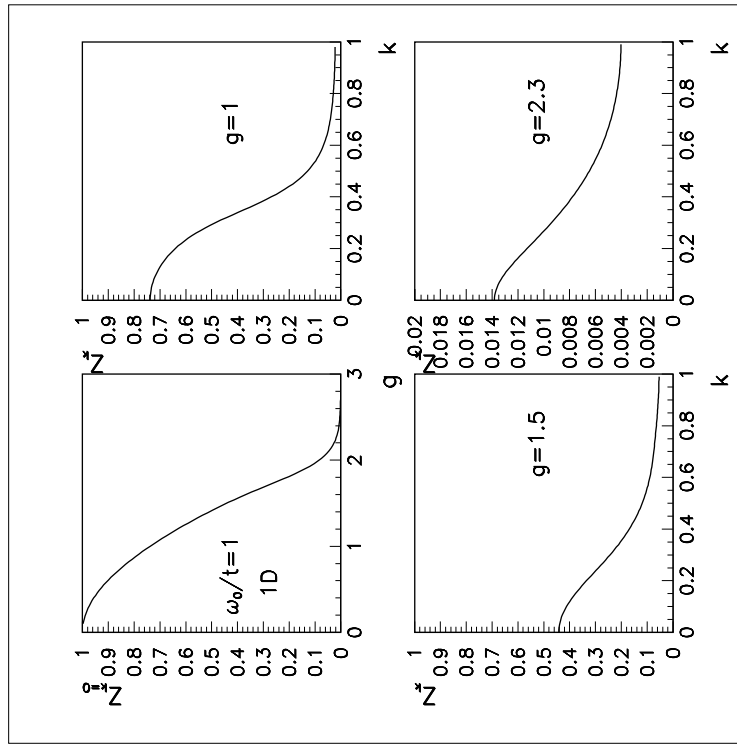


FIG. 6. The spectral weight of the polaronic ground state in one dimension as a function of the electron-phonon coupling constant at  $k = 0$  (Fig.6a.) and as a function of the polaron Bloch state wavenumber (in units of  $\pi/a$ ) for different values of  $g$  (Fig.6b., Fig.6c. and Fig.6d.) at  $\omega_0/t = 1$ .

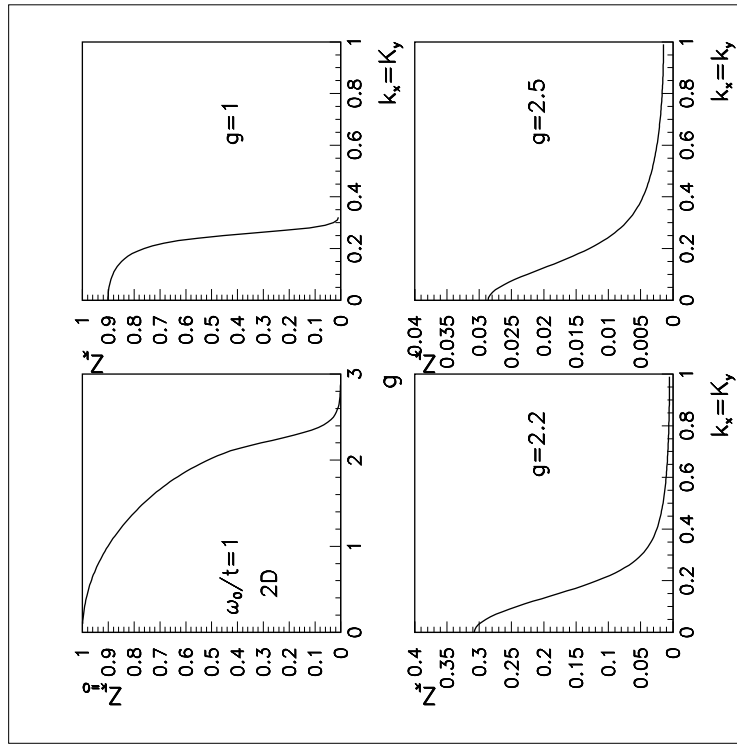


FIG. 7. The spectral weight of the polaronic ground state in two dimensions as a function of the electron-phonon coupling constant at  $k = 0$  (Fig.7a.) and as a function of the polaron Bloch state wavenumber (in units of  $\pi/a$ ) for different values of  $g$  (Fig.7b., Fig.7c. and Fig.7d.) at  $\omega_0/t = 1$ .

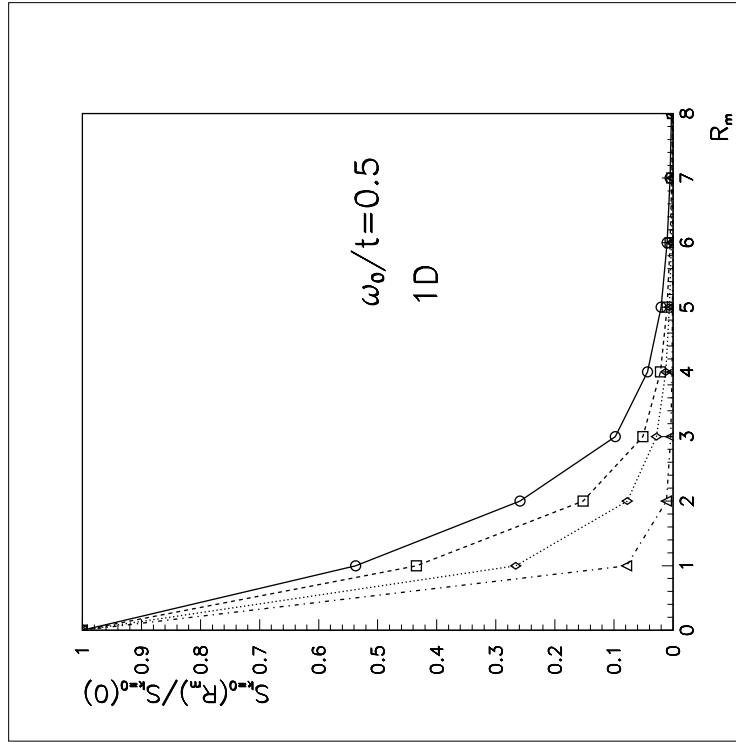


FIG. 8. The dimensionless quantity  $S_{\vec{k}}(\vec{R}_m)$ , at  $\omega_0/t = 0.5$  and in one dimension, for different values of the electron-phonon coupling constant at  $\vec{k} = 0$ :  $g = 1$  (circles),  $g = 2$  (squares),  $g = 2.2$  (diamonds),  $g = 2.5$  (triangles).